Shoulder Overload Monitoring for Upper-Limb Prosthesis

Stephanie Akakabota & Eins Besmanos
BioE 105 (Introduction to Medical Devices) Final Project

1 Introduction

A 2024 study estimates that over 212,000 individuals in the United States are living with upper limb loss, (Rivera et al., 2024). For people with upper limb amputation (ULA), prosthetic rehabilitative care can quality of life, improve mental health, and improve independence with daily tasks, however body-powered and myoelectric prostheses report a staggeringly high abandonment rate (26 % and 23 % respectively), with little to no improvements over the last decade (Resnik et al., 2023; Biddiss et al., 2022). Studies report a ~ 30 % prevalence of shoulder pain in adults with ULA mainly due to awkward compensatory movements made to operate prostheses, a problem that current research (mainly aimed to improve function and fit at the socket) aren't addressing (Webster et al., 2022; Tiesler et al., 2025). We propose a shoulder monitoring system combining surface electromyography (sEMG) with an inertial measurement unit to help clinicians observe shoulder activation and torque during everyday use. With simulated trials demonstrating a robust system with clear feedback to warn users of dangerous movement patterns and a U.S. intelligent prosthetics expected to rise from $313 million to over $550 million in the next ten years, the adoption of this product would be marketable and effective (Insights, 2025).

2 Background and Significance

People with ULA frequently develop musculoskeletal problems in the shoulder on the prosthetic side, due to awkward postures and compensatory positions to use their device. About 1/3 of users with ULA experiencing significant shoulder pain, a symptom that has a 1.05 odds of worsening with each year post amputation (Webster et al., 2022). A study found 57% Norwegian adults with reported neck or upper-back pain compared to a control group (Østlie et al., 2011). With a large fraction of upper-limb prostheses being (over 23 %), with users citing discomfort, functionality, and fatigue, as key reasons for abandonment, current assessments of shoulder injury or overload mostly rely on questionnaires and clinical assessments occuring after chronic pain or injury has already developed (Resnik et al., 2023; Østlie et al., 2011). These methods cannot measure mechanical load in real time and cannot warn users of imminent injury.

Engineering developments mainly focus on improving control or improving socket alignment/pressure to address discomfort. State-of-the-art myoelectric prosthetics use electromyogram (EMG) pattern recognition to track the EMG patterns from multiple residual limb muscles to determine user's gesture/grip intent(Resnik et al., 2018). While highly accurate ($> 90\%$), this cannot be used as a diagnostic marker to measure muscular overload or predict injury. Additionally, current strap pressure systems use Flexiforce A401-25 sensors measuring $0 \rightarrow 111$N , corresponding to pressures as low as 15 mmHg over a 0.203 mm contact area with high linearity ($R^2 \approx 0.98$) and a sensor bandwidth of ~ 3 Hz (Tamez-Duque et al., 2015). These sensors can trigger safety warnings for unsafe skin pressure (> 2000mmHg. While this can address skin sores and breakage, socket pressure studies are not targeted at joint overuse and chronic injury prevention. The missing biosignal that could address this is a combination of EMG, socket force, and limb orientation, creating an overuse threshold for shoulder torque that can warn users about prosthetic position before pain and joint damage occurs.

3 Biosignal Definition and Background Data

3.1 Signal Description

Our device will measure surface electromyography (sEMG), electrical signal that reflect activation from the anterior deltoid and trapezius muscles. Following the data processing procedure in Klich et al. (2021), raw sEMG data will be taken from each region(a noisy measurement oscillating around 0V with peak to peak amplitudes of $0.1 \rightarrow 5mV$). For each muscle, the signal is band-pass filtered to a $20 \rightarrow 500$ Hz bandwidth, amplified, then rectified and placed through a digital low-pass filter (Klich et al., 2021). The channel with the larger EMG value at each time step will be taken as the dominant representation of shoulder activation, a value that is then normalized by the users' max voluntary contraction (% MVC), calculated via a 5 second calibration hold. Every day tasks will sit around $10\% \rightarrow 30\%$MVC, with any flags $> 60\%$ indicating shoulder health risk, since shoulder EMG amplitudes that are high for long periods of time indicate fatigue and overuse risk (Klich et al., 2021).

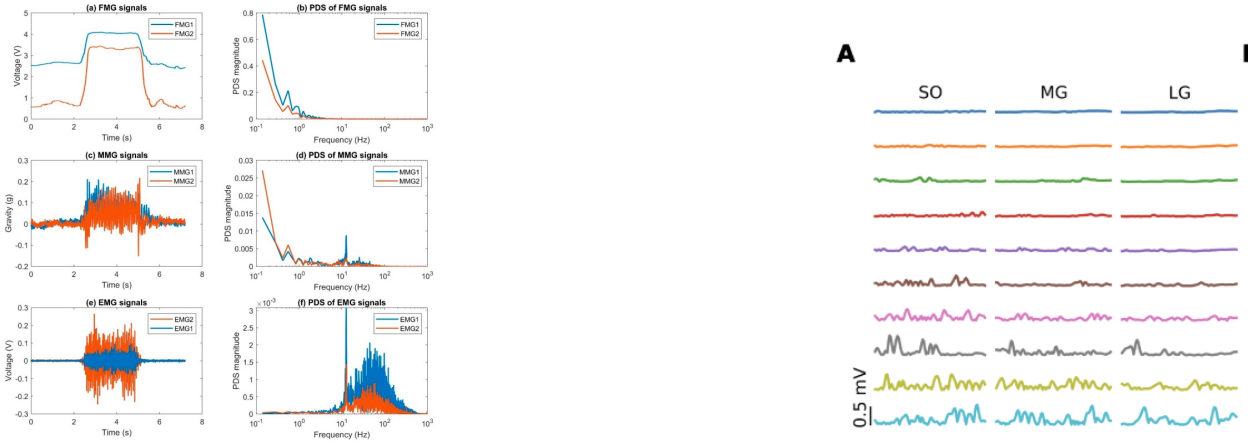

Figure 1. (Time-domain FSR, MMG, and EMG signals and corresponding power spectra (left), and example RMS sEMG snippets at different percentages of MVC from three lower-leg muscles (right), illustrating relevant bandwidth and MVC-normalized amplitude behavior (Diong et al., 2022).

3.2 Background Data

The left figure of Figure 1 shows the time domain and frequency spectum signal during an isometric contraction from two sensors placed at the top and bottom of the forearm. This indicates desired sEMG signal, and concomitant mechanomyography (MMG) muscle vibration and FMG mechanical signals. We can see that the FMG signal occurs typically around < 10 Hz, and MMG ($10 \rightarrow 100$ Hz) and EMG ($10 \rightarrow 1000$ Hz), mostly falling in the $400 \rightarrow 500$ Hz range, guiding our filter design.

The right of figure 1 shows example EMG amplitudes for root-mean-square values for 50 ms windows taken from 3 muscle groups at different contraction efforts, from $0\% \rightarrow 100\%$ MVC. The amplitudes increase to about .,5 mV as effort increases form top to bottom.

4 Hardware

4.1 sEMG

The sEMG has two Ag/AgCl electrodes attached to the anterior deltoid and upper trapezius along their muscle fibers (see **??**). These are connected to the inverting and non-inverting inputs of an INA118 differential amplifier, shown in the circuit diagram in Figure 2. A third Ag/AgCl reference electrode placed on a neutral location of the body, as a ground reference, connected to the to the INA118 Ref pin (Electrode 3, body ground).

The amplifier uses a gain resistor $R_g = 500\ \Omega$ to create a voltage gain

$$G = 1 + \frac{50\ k\Omega}{R_g} = 1 + \frac{50\ k\Omega}{500\ \Omega} = 101.$$

The INA118 output then passes through a cascaded high-pass and low-pass stage, forming a band-pass filter with

$$f_L = \frac{1}{2\pi R_3 C_1} \approx 20\ \text{Hz}, \quad f_H = \frac{1}{2\pi R_4 C_2} \approx 500\ \text{Hz},$$

where $C_1 = 0.82\ \mu$F, $R_3 = 10\ k\Omega$, $R_4 = 3.3\ k\Omega$, and $C_2 = 0.1\ \mu$F. The filtered output converts a 0.1–5 mV differential sEMG signal into a 0–5 V signal band-limited to 20–500 Hz for post-processing by the Arduino Nano through input A0.

4.2 Dual IMU

The second stage contains a MPU-6050 IMU mounted to lateral upper arm, so that the sensor's z-axis aligns with the gravity vector when the arm hangs neutrally. The IMU receives power from the Arduino Nano $+3.3$V pin, and is connected to a common ground with the rest of the circuit. It's SDA and SCL pins each connect to Arduino A4 and A5 pins, respectively, and a $4.7k$ pull up resistor. The accelerometer provides 3-axis acceleration, which is read and converted onboard to an upper arm elevation angle $\theta_{\text{UA}}(t)$. This angle, combined with an estimated mass of prosthesis and center-of-mass distance will be used to calculate the shoulder moment arm and torque in post processing. Arduino power comes from a $5V$ Li-Po battery.

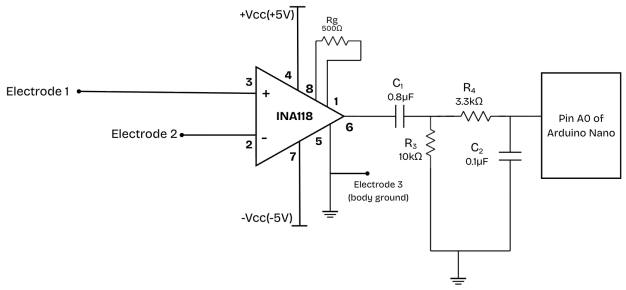

Figure 2. Circuit Schematic of sEMG electrodes, amplified by op amp and put through bandpass filter.

4.3 Diagnostic Procedure

Before measurement, patient is notified of the procedure and consent is given. The skin of the anterior deltoid, upper trapezius, and a bony reference zone is cleaned, and two Ag/AgCl sEmg electrodes and one reference electrode are attached. The upper-arm and forearm IMUs are connected and aligned to the respective limbs along the z-axis. The subject will stand neutrally to calculate zero angles, and then will perform a maximum voluntary contraction for 5 seconds to determine 100 % MVC.

5 Post Processing

First, the 5 second MVC trial described in the diagnostic procedure will be cleaned through rectification and a digital low-pass filter, and the peak value $e_{\text{MVC,max}}$ will be recorded from the upper trapezius electrode.

Figure 3 shows the simulation of this process (see code in appendix), with a simulated 5 sec contraction from the diagnostic procedure, with added noise and an 80 Hz carrier wave, the signal after low-pass filtering and rectification, and finally the normalization by Max Voluntary Contraction with a reported 100% MVC value:

Second, during continuous monitoring, raw sEMG signals from both the upper trapezius (UT) and anterior deltoid (AD) electrodes will be cleaned through rectification and a 5 Hz digital low-pass filter, making two EMG envelopes: $e_{\text{env,UT}}(t)$ and $e_{\text{env,AD}}(t)$, a method described by (Klich et al., 2021). The dominant EMG will represent the signal change over time:

$$e_{\text{env}}(t) = \text{LPF}_{5\text{Hz}}\big(\max(|e_{\text{raw,UT}}(t)|, |e_{\text{raw,AD}}(t)|)\big). \tag{1}$$

This gets normalized to the max %MVC $e_{\text{MVC,max}}$:

$$\%\text{MVC}(t) = 100 \cdot \frac{e_{\text{env}}(t)}{e_{\text{MVC,max,UT}}}. \tag{2}$$

The raw 3-axis accelerometer data from the upper arm IMU is converted to voltage through the on-board ADC, providing anan upper arm elevation angle $\theta_{\text{UA}}(t)$ relative to the gravithy vector using the vertical acceleration component: $\theta_{\text{UA}}(t) = \arcsin\left(\frac{a_{z,\text{clean}}(t)}{g}\right)$ where $a_z(t)$ is the accelerometer's vertical component, measuring the angle of the upper arm from the shoulder's center of mass. When the shoulder is relaxed at its side, $\theta_{\text{UA}} = 0^\circ$), and when fully abducted,($\theta_{\text{UA}} = 90^\circ$).

A 2 Hz digital low-pass filter is applied to the signal giving a cleaned $\theta_{\text{UA}}(t)$ and estimated prosthesis mass $m_p = 1.5$ kg with center-of-mass distance $L_p = 0.35$ m compute shoulder moment arm $L_\perp(t) = L_p \sin\big(\theta_{\text{UA}}(t)\big)$ and torque $\tau_{\text{shoulder}}(t) = m_p g\, L_\perp(t)$, where $g = 9.81$ m/s^2.

At each 50 Hz time step, $\tau_{\text{shoulder}}(t)$ and $\%\text{MVC}(t)$ are compared to thresholds $\tau_{\text{th}} = 60\%\tau_{\text{max}}$ and $M_{\text{th}} = 60\%$. An overload flag $F(t)$ is triggered when:

$$F(t) = \begin{cases} 1, & \text{if } \tau_{\text{shoulder}}(t) > \tau_{\text{th}} \text{ or } \%\text{MVC}(t) > M_{\text{th}}, \\ 0, & \text{otherwise.} \end{cases} \tag{3}$$

6 Anticipated Outcomes

6.1 Prediction

Based on preliminary data, we expect this device to produce varied voltage readings over time. There will be relatively low % MVC and torque during most daily tasks, with brief peaks when grabbing objects overhead or misjudgments of an objects weight distribution, causing a compensatory adjustment. This would appear as long periods with no overuse warning, with the occasional

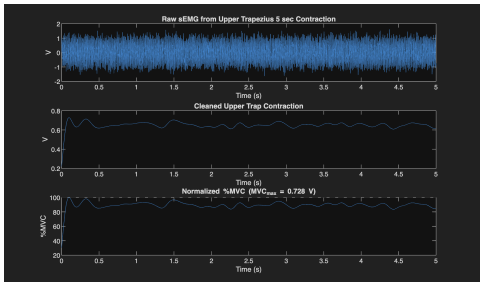

Figure 3. Raw sEMG from upper trapezius Contraction trial(top), Cleaned signal (middle), normalized %MVC signal with max value (bottom).

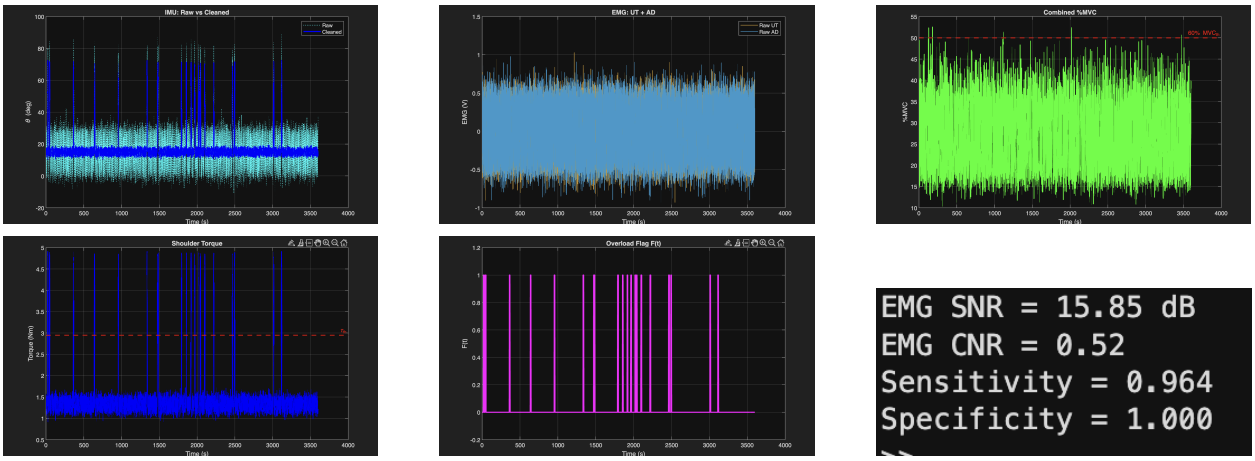

Figure 4. (top row) Simulated raw vs. cleaned IMU shoulder angle, raw dual-electrode sEMG, and combined %MVC, and (bottom row) shoulder torque with threshold, overload flag $F(t)$, and summary performance metrics (SNR, CNR, sensitivity, specificity) derived from the same data.

short stretches of overuse warning. A clinician could then view overload exposure during the rehabilitation process and assess progress.

6.2 Simulated Trials

Through upper arm angle kinematic studies, we have simulated one hour of prosthesis use to demonstrate the device output over time, sampled at 50 Hz. Figure x shows simulated raw sEMG signals and their corresponding cleaned data.

The hour data contains low angles and higher angles simulating grasping, overhead reaching, and general body movement within an hour. These values are normalized by the reported MVC_{max} value from the 5 second contraction, and figure x shows that hour long data as a percent of the max voluntary contraction.

IMU data is simulated with an additional $\sim$ 3 degrees of noise to create a realistic output. This data is smoothed through a 2 Hz cutoff low pass filter.

The shoulder angle is then converted to torque. The degrees are converted to radians, and the corresponding perpendicular moment arm is calculated from equations 3 and 4. Lp = estimated distance from shoulder to prosthesis center of mass.

The maximum torque seen over the hour is found, and the threshold τ_{th} is set at 60 % of that value.

Overload is defined from the EMG when % MVC is above its threshold value, or if torque rises above τ_{th}. The overload flag F_{clean} is 1 whenever either case is true, otherwise 0, as shown in equation 5.

Figure 4 shows the three main figures created from this:

(i) Raw vs. cleaned shoulder angle over the hour
(ii) Combined Upper Trapezius and Anterior Deltoid EMG over the hour
(iii) Combined % MVC contraction
(iv) Torque over the hour with the threshold line
(v) Response of the torque overload flag.

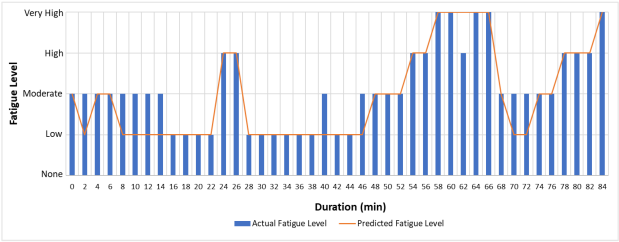

Figure 5. Predicted and actual fatigue level for every two-min on the unseen dataset. Bangaru et al. (2022)

6.3 SNR and CNR Calculation

From the cleaned EMG data, a signal-to-noise ratio is calculated as $\text{SNRdB} = 20\log_{10}\left(\frac{\mu_{\text{high}}}{\sigma_{\text{rest}}}\right)$, with high effort periods defined as $\%\text{MVC} > 45\%$, low effort periods defined as $\%\text{MVC} < 10\%$, μ_{signal} defined as the signal average during peaks, and σ_{rest} defined as the standard deviation during rest. The contrast-to-noise ratio is defined as: $\text{CNR} = \frac{|\mu_{\text{high}} - \mu_{\text{low}}|}{\sqrt{\sigma^2_{\text{low}} + \sigma^2_{\text{high}}}}$

between high loads ($> 45\%$) and low loads ($10\% \rightarrow 35\%$).

6.4 Sensitivity

Sensitivity is calculated by comparing the algorithm's decisions of overload at 60 % to a true overload value $GT(t) = 1$ which is defined by 45% MVC or 55% τ_{max}. The amount of True Positives (TP = $F_{\text{alg}}(t) = 1$ and $GT(t) = 1$) and False Negatives (FN = $F_{\text{alg}}(t) = 0$ and $GT(t) = 1$) makeup the following equations:

$$\text{Sensitivity} = \frac{\text{TP}}{\text{TP} + \text{FN}} = 0.964 \tag{4}$$

$$\text{Specificity} = \frac{\text{TN}}{\text{TN} + \text{FP}} = 1.000 \tag{5}$$

The printed numbers in Figure 4 give device performance metrics from the simulated data.

6.5 Comparison

The Simulated SNR of **15.85** dB exceeds the minimum value for reliable sEMG 5.51 dB, and exceeds the desirable SNR of 12.28 by 29 % (Rojas et al., 2018). While sEMG studies are done with regards to prosthetic shoulder pain, sEMG sensitivity for lower back pain studies is reported to be between $76 \rightarrow 100$ percent (Farina et al., 2003).

7 Competing Technology

DorsaVi, a company that combines EMG and motion sensing for their advanced wearable sensors, monitors athletic movement analysis or workplace safety that measure precise biomechanical activity. They ensure ergonomic wellness by having their sensors track muscular load and fatigue during advanced movements to reduce the risk of injury. Their system was developed based on a fatigue monitor for construction workers using forearm EMG and IMU data with an accuracy of 92.31% when assessing their fatigue level compared to their heart rate, showcasing that these sensors work for active monitoring, (Bangaru et al., 2022). However, these solutions focus on generalized ergonomic assessments. Our idea uniquely targets shoulder torque estimation using EMG and IMU orientation data for upper-limb prosthesis that addresses shoulder pain. This enables proactive fatigue detection during daily prosthesis use, providing immediate feedback that existing companies have not covered.

8 Money

Our device targets a market consisting of upper-limb prosthesis users who experience shoulder discomfort during daily use, estimated to be over 200,000 individuals in the United States, (Rivera et al., 2024). Assuming a consumer market of 1% by year one, 3% by year three, and 7% by year five, the device could reach approximately 2,000 users initially and over 14,000 users by the fifth year. The estimated cost of materials per unit is approximately $85 to $120, which include the EMG electrodes, the amplifiers, and the IMUs. Accounting for assembly, regulatory, software costs, and insurance per unit production can be estimated at $200. The competing wearable sensor devices retail between $700 to $1,5000. For an EMG armband sensor that has all the necessary EMG electrodes and amplifiers included, Mindrove sells a unit for $729, (Mindrove, 2024). If we sell our device for $750, this allows us to gain a profit that benefits from the strong margin while remaining an accessible add-on for existing prostheses. Our product is attractive to early-stage investors due to the low manufacturing cost, non-invasive design, unique yet clinical need, and ability to advance as technology evolves.

Appendix A: Simulation and Analysis Code

```
%% =========================
%  A) 5 s MVC BENCHMARK TRIAL
% ==========================
fs_mvc = 1000;
T_mvc  = 5;
t_mvc  = (0:1/fs_mvc:T_mvc-1/fs_mvc)';

env_UT_mvc = 1.0 + 0.1*randn(size(t_mvc));
fc = 80;
carrier = sin(2*pi*fc*t_mvc);
raw_UT_mvc = env_UT_mvc .* carrier + 0.2*randn(size(t_mvc));

emg_rect_UT_mvc = abs(raw_UT_mvc);
lpFilt_mvc = designfilt('lowpassiir','FilterOrder',4, ...
                'HalfPowerFrequency',5,'SampleRate',fs_mvc);
emg_env_UT_mvc = filtfilt(lpFilt_mvc, emg_rect_UT_mvc);

MVC_max_UT = max(emg_env_UT_mvc);
pct_MVC_mvc = 100 * emg_env_UT_mvc / MVC_max_UT;

figure(1);
subplot(3,1,1);
plot(t_mvc, raw_UT_mvc);
xlabel('Time (s)'); ylabel('V');
title('Raw sEMG from Upper Trapezius 5 s Contraction');

subplot(3,1,2);
plot(t_mvc, emg_env_UT_mvc);
xlabel('Time (s)'); ylabel('V');
title('Cleaned Upper Trap Contraction');

subplot(3,1,3);
plot(t_mvc, pct_MVC_mvc);
xlabel('Time (s)'); ylabel('%MVC');
title(sprintf('Normalized %%MVC (MVC_{max} = %.3f V)', MVC_max_UT));
yline(100,'k--','100%% MVC');

%% =========================
%  B) 1-HOUR SIMULATED DAILY USE - TWO ELECTRODES
% ==========================
fs = 50;
T  = 3600;
t  = (0:1/fs:T-1/fs)';

mp = 1.5;      % prosthesis mass [kg]
Lp = 0.35;     % COM distance [m]
g  = 9.81;     % gravity [m/s^2]

MVC_th      = 60;    % %MVC threshold for algorithm
tau_frac_th = 0.60;  % torque threshold fraction
```

```
theta_true_deg = 15 + 5*randn(size(t));
nBursts = 20;
for k = 1:nBursts
    t0  = randi([1, T-20]);
    idx = (t >= t0) & (t <= t0+10);
    theta_true_deg(idx) = 30 + 40*sin(pi*(t(idx)-t0)/10) + 5*randn(sum(idx),1);
end

% TWO ELECTRODE ENVELOPES (TRUE)
env_UT_true = 0.1 + 0.002*max(theta_true_deg,0) + 0.04*randn(size(t));
env_AD_true = 0.1 + 0.004*max(theta_true_deg,0) + 0.06*randn(size(t));
env_UT_true(env_UT_true < 0) = 0;
env_AD_true(env_AD_true < 0) = 0;

pctMVC_UT_true = 100 * env_UT_true / MVC_max_UT;

% RAW MEASUREMENTS
theta_raw_deg = theta_true_deg + 3*randn(size(t));
raw_UT_meas   = env_UT_true .* sin(2*pi*80*t) + 0.18*randn(size(t));
raw_AD_meas   = env_AD_true .* sin(2*pi*75*t) + 0.22*randn(size(t));

% CLEANING
win_imu = round(fs/2);
theta_clean_deg = movmean(theta_raw_deg, win_imu);

win_emg = round(fs/5);
UT_rect = abs(raw_UT_meas);
AD_rect = abs(raw_AD_meas);
env_UT_clean = movmean(UT_rect, win_emg);
env_AD_clean = movmean(AD_rect, win_emg);

% COMBINED ENVELOPE
env_hour_clean    = max(env_UT_clean, env_AD_clean);
pctMVC_hour_clean = 100 * env_hour_clean / MVC_max_UT;

% TORQUE (FROM CLEANED ANGLE)
theta_clean_rad = deg2rad(theta_clean_deg);
Lperp_clean     = Lp .* sin(theta_clean_rad);
tau_clean       = mp * g .* Lperp_clean;

tau_max_est = max(tau_clean);
tau_th      = tau_frac_th * tau_max_est;

% ALGORITHM OVERLOAD FLAG
Over_MVC_alg = pctMVC_hour_clean > MVC_th;
Over_tau_alg = tau_clean         > tau_th;
F_alg        = Over_MVC_alg | Over_tau_alg;

%% ========================
%  C) SNR/CNR FROM CLEANED COMBINED EMG
% ========================
rest_idx  = pctMVC_UT_true < 10;
```

```
low_idx   = (pctMVC_UT_true >= 10) & (pctMVC_UT_true <= 35);
high_idx  = pctMVC_UT_true > 45;

mu_signal   = mean(env_hour_clean(high_idx));
sigma_noise = std(env_hour_clean(rest_idx));
SNR_linear  = mu_signal / sigma_noise;
SNR_dB      = 20*log10(SNR_linear);

mu_low    = mean(env_hour_clean(low_idx));
mu_high   = mean(env_hour_clean(high_idx));
sigma_low  = std(env_hour_clean(low_idx));
sigma_high = std(env_hour_clean(high_idx));
CNR        = abs(mu_high - mu_low) / sqrt(sigma_low^2 + sigma_high^2);

fprintf('EMG SNR = %.2f dB\n', SNR_dB);
fprintf('EMG CNR = %.2f\n',    CNR);

%% =========================
%  D) SENSITIVITY/SPECIFICITY
% =========================
MVC_true_th = 45;
tau_true_th = 0.55 * tau_max_est;

GT = (pctMVC_UT_true > MVC_true_th) | (tau_clean > tau_true_th);

TP = sum(F_alg &  GT);
FP = sum(F_alg & ~GT);
TN = sum(~F_alg & ~GT);
FN = sum(~F_alg &  GT);

sensitivity = TP / (TP + FN);
specificity = TN / (TN + FP);

fprintf('Sensitivity = %.3f\n', sensitivity);
fprintf('Specificity = %.3f\n', specificity);

%% =========================
%  E) 1-HOUR FIGURES
% =========================
figure(2);
plot(t, theta_raw_deg,'c:','LineWidth',1); hold on;
plot(t, theta_clean_deg,'b','LineWidth',2);
xlabel('Time (s)'); ylabel('\theta (deg)');
title('IMU: Raw vs Cleaned');
legend('Raw','Cleaned'); grid on;

figure(3);
plot(t, raw_UT_meas,'color',[0.8 0.6 0.2],'LineWidth',1); hold on;
plot(t, raw_AD_meas,'color',[0.2 0.6 0.8],'LineWidth',1);
xlabel('Time (s)'); ylabel('EMG (V)');
title('EMG: UT + AD');
legend('Raw UT','Raw AD'); grid on;
```

```
figure(4);
plot(t, pctMVC_hour_clean,'g','LineWidth',1.5); hold on;
yline(MVC_th,'r--','60% MVC_{th}','LineWidth',2);
xlabel('Time (s)'); ylabel('%MVC');
title('Combined %MVC'); grid on;

figure(5);
plot(t, tau_clean,'b','LineWidth',1.5); hold on;
yline(tau_th,'r--','\tau_{th}','LineWidth',2);
xlabel('Time (s)'); ylabel('Torque (Nm)');
title('Shoulder Torque'); grid on;

figure(6);
plot(t, double(F_alg),'m','LineWidth',2);
ylim([-0.2 1.2]);
xlabel('Time (s)'); ylabel('F(t)');
title('Overload Flag F(t)'); grid on;
```

REFERENCES

Bangaru, S. S., C. Wang, and F. Aghazadeh, 2022, Automated and continuous fatigue monitoring in construction workers using forearm emg and imu wearable sensors and recurrent neural network: Sensors, **22**, 9729.

Biddiss, E., D. G. Smith, T. Chau, et al., 2022, Current rates of prosthetic usage in upper-limb amputees – have innovations had an impact on device acceptance?: Disability and Rehabilitation.

Diong, J., K. C. Kishimoto, J. E. Butler, and M. E. Héroux, 2022, Muscle electromyographic activity normalized to maximal muscle activity, not to mmax, better represents voluntary activation: PLOS ONE, **17**, e0277947.

Farina, D., M. Gazzoni, and R. Merletti, 2003, Assessment of low back muscle fatigue by surface emg signal analysis: methodological aspects: Journal of Electromyography and Kinesiology, **13**, 319–332.

Insights, F. M., 2025, Demand for intelligent prosthetics in USA | global market analysis report - 2035: https://www.futuremarketinsights.com/reports/united-states-intelligent-prosthetics-market. (Accessed 12 December 2025).

Klich, S., A. Kawczyński, B. Pietraszewski, M. Zago, A. Chen, M. Smoter, H. Hassanlouei, and N. Lovecchio, 2021, Electromyographic evaluation of the shoulder muscle after a fatiguing isokinetic protocol in recreational overhead athletes: International Journal of Environmental Research and Public Health, **18**, 2516.

Mindrove, 2024, Emg armband — 8 channel: https://mindrove.com/product/emg-armband/. (Accessed: 14 December 2025).

Resnik, L., H. H. Huang, A. Winslow, D. L. Crouch, F. Zhang, and N. Wolk, 2018, Evaluation of emg pattern recognition for upper limb prosthesis control: a case study in comparison with direct myoelectric control: Journal of NeuroEngineering and Rehabilitation, **15**, 23.

Resnik, L. J., M. L. Borgia, and M. A. Clark, 2023, Prevalence and predictors of unmet need for upper-limb prostheses: an observational cohort study: J. Prosthet. Orthot., **36**, 80–88.

Rivera, J. A., K. Churovich, A. B. Anderson, and B. K. Potter, 2024, Estimating recent us limb loss prevalence and updating future projections: Arch. Rehabil. Res. Clin. Transl., **6**, 100376.

Rojas, A., A. Farfan, E. Mora, L. I. Minchala, and S. Wong, 2018, Assessing the snr influence in the estimation of the mean frequency of lower limbs semg signals: IEEE Latin America Transactions, **16**, 2108–2114.

Tamez-Duque, J., R. Cobian-Ugalde, A. Kilicarslan, A. Venkatakrishnan, R. Soto, and J. L. Contreras-Vidal, 2015, Real-time strap pressure sensor system for powered exoskeletons: Sensors, **15**, 4550–4563.

Tiesler, L. M., M. Edel, F. Wang, P. Pieroh, W.-G. Drossel, A. Carabello, D. Zipplies, C.-E. Heyde, and S. Schleifenbaum, 2025, Objective measurement methods for the evaluation of socket comfort in patients with transfemoral amputation: a systematic review: Frontiers in Bioengineering and Biotechnology, **13**, 1576729.

Webster, J. B., N. Webster, M. Borgia, and L. Resnik, 2022, Frequency, severity, and implications of shoulder pain in people with major upper limb amputation who use prostheses: Results of a national study: PM&R, **14**, 901–912.

Østlie, K., R. J. Franklin, O. H. Skjeldal, A. Skrondal, and P. Magnus, 2011, Musculoskeletal pain and overuse syndromes in adult acquired major upper-limb amputees: Archives of Physical Medicine and Rehabilitation, **92**, 1967–1973.e1.